





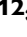


Myeloid CD40 deficiency reduces atherosclerosis by impairing macrophages' transition into a pro-inflammatory state

Laura A. Bosmans ¹, Claudia M. van Tiel¹, Suzanne A. B. M. Aarts¹, Lisa Willemsen ¹, Jeroen Baardman ¹, Bram W. van Os¹, Myrthe den Toom¹, Linda Beckers¹, David J. Ahern², Johannes H.M. Levels³, Aldo Jongejan⁴, Perry D. Moerland⁴, Sanne G.S. Verberk⁵, Jan van den Bossche ^{1,5}, Menno M. P. J. de Winther¹, Christian Weber ^{6,7,8,9}, Dorothee Atzler^{6,9,10}, Claudia Monaco ², Norbert Gerdes¹¹, Annelie Shami ^{1,12*†}, and Esther Lutgens^{1,6,7,13†}

¹Department of Medical Biochemistry, Amsterdam Cardiovascular Sciences (ACS) & Amsterdam Infection and Immunity (All), Amsterdam University Medical Centres, University of Amsterdam, Amsterdam, The Netherlands; ²Kennedy Institute of Rheumatology, Nuffield Department of Orthopaedics, Rheumatology and Musculoskeletal Sciences, University of Oxford, Oxford, UK; ³Department of Vascular Medicine, Amsterdam Cardiovascular Sciences (ACS), Amsterdam University Medical Centres, University of Amsterdam, Amsterdam, The Netherlands; ⁴Bioinformatics Laboratory, Department of Epidemiology and Data Science, Amsterdam UMC, University of Amsterdam, Amsterdam, The Netherlands; ⁵Department of Molecular Cell Biology and Immunology, Amsterdam Cardiovascular Sciences, Cancer Center Amsterdam, Amsterdam UMC, Vrije Universiteit Amsterdam, Amsterdam, Netherlands; ⁶Institute of Cardiovascular Prevention (IPEK), Ludwig Maximilian's University, Munich, Germany; ⁷German Centre for Cardiovascular Research (DZHK), partner site Munich Heart Alliance, Munich, Germany; ⁸Department of Biochemistry, Cardiovascular Research Institute Maastricht (CARIM), Maastricht University, Maastricht, the Netherlands; ⁹Munich Cluster for Systems Neurology (SyNergy), Munich, Germany; ¹⁰Walter-Straub-Institute of Pharmacology and Toxicology, Ludwig-Maximilians Universität, München, Germany; ¹¹Division of Cardiology, Pulmonology and Vascular Medicine, Medical Faculty, University Hospital and Heinrich Heine University Düsseldorf, Germany; ¹²Department of Clinical Sciences Malmö, Lund University, Clinical Research Center, Malmö, Sweden; and ¹³Experimental Cardiovascular Immunology Laboratory, Department of Cardiovascular Medicine, Mayo Clinic, Rochester, MN, USA

Received 16 February 2022; revised 20 April 2022; accepted 4 May 2022; online publish-ahead-of-print 19 May 2022

Aims

CD40 and its ligand, CD40L, play a critical role in driving atherosclerotic plaque development. Disrupted CD40-signalling reduces experimental atherosclerosis and induces a favourable stable plaque phenotype. We recently showed that small molecule-based inhibition of CD40-tumour necrosis factor receptor associated factor-6 interactions attenuates atherosclerosis in hyperlipidaemic mice via macrophage-driven mechanisms. The present study aims to detail the function of myeloid CD40 in atherosclerosis using myeloid-specific CD40-deficient mice.

Method and Results

Cd40^{flox/flox} and *LysM-cre Cd40^{flox/flox}* mice on an *Apoe^{-/-}* background were generated (*CD40^{wt}* and *CD40^{mac-/-}*, respectively). Atherosclerotic lesion size, as well as plaque macrophage content, was reduced in *CD40^{mac-/-}* compared to *CD40^{wt}* mice, and their plaques displayed a reduction in necrotic core size. Transcriptomics analysis of the *CD40^{mac-/-}* atherosclerotic aorta revealed downregulated pathways of immune pathways and inflammatory responses. Loss of CD40 in macrophages changed the representation of aortic macrophage subsets. Mass cytometry analysis revealed a higher content of a subset of alternative or resident-like *CD206⁺CD209b⁻* macrophages in the atherosclerotic aorta of *CD40^{mac-/-}* compared to *CD40^{wt}* mice. RNA-sequencing of bone marrow-derived macrophages of *CD40^{mac-/-}* mice demonstrated upregulation of genes associated with alternatively activated macrophages (including *Fcrl2*, *Thbs1*, *Sdc1*, and *Tns1*).

Conclusions

We here show that absence of CD40 signalling in myeloid cells reduces atherosclerosis and limits systemic inflammation by preventing a shift in macrophage polarization towards pro-inflammatory states. Our study confirms the merit of macrophage-targeted inhibition of CD40 as a valuable therapeutic strategy to combat atherosclerosis.

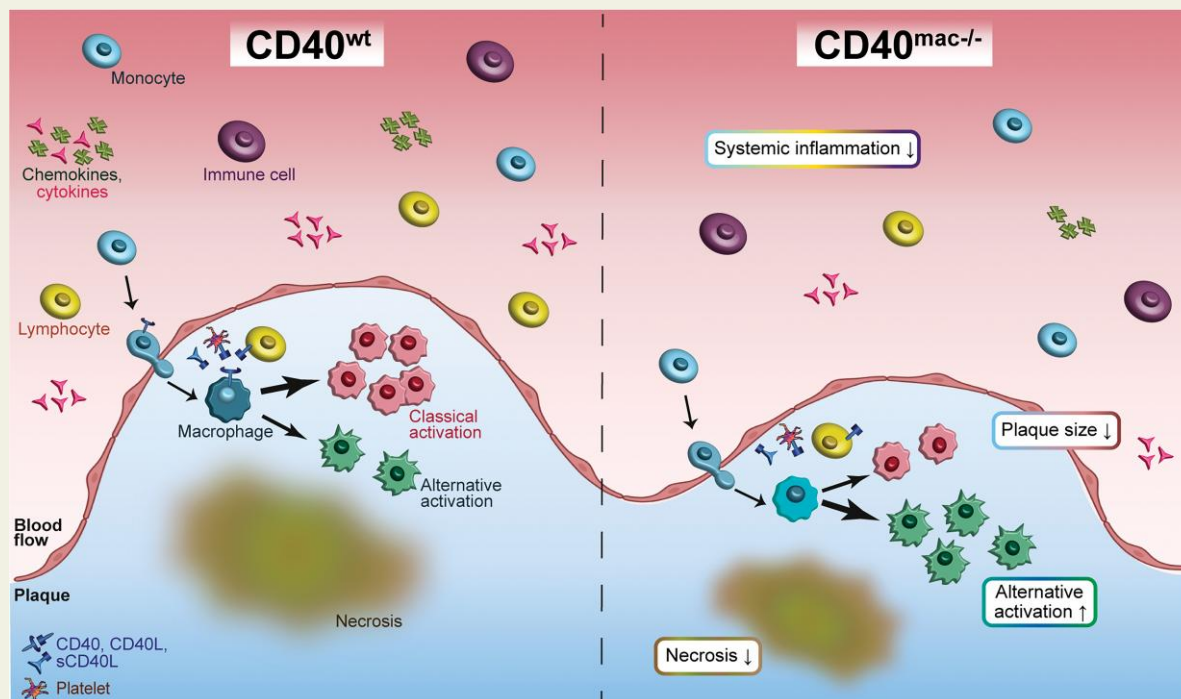
* Corresponding author. Tel: +46 (0)40 391206, E-mail: annelie.shami@med.lu.se

† A.S. and E.L. contributed equally.

© The Author(s) 2022. Published by Oxford University Press on behalf of the European Society of Cardiology.

This is an Open Access article distributed under the terms of the Creative Commons Attribution-NonCommercial License (<https://creativecommons.org/licenses/by-nc/4.0/>), which permits non-commercial re-use, distribution, and reproduction in any medium, provided the original work is properly cited. For commercial re-use, please contact journals.permissions@oup.com

Graphical Abstract



Keywords

Atherosclerosis • CD40 • Macrophage • Inflammation

1. Introduction

Atherosclerosis—a chronic, lipid driven inflammatory disease of the arterial wall—is the major underlying cause of cardiovascular disease (CVD)¹ and the number one cause of death worldwide accounting for 7.4 million deaths per year.² Although lipid lowering strategies have been considered ‘standard of care’ for many years, recent clinical trials have revealed the potential of immuno-therapies to combat CVD. The outcomes of the Canakinumab Anti-Inflammatory Thrombosis Outcome Study,³ Colchicine Cardiovascular Outcome Trial, and low dose colchicine (LoDoCo1 and LoDoCo2) clinical trials^{4–6} show that drugs targeting the interleukin (IL)-1 β /inflammasome pathway are successful in reducing the risk of (recurrent) cardiovascular events, but not in reducing mortality. In order to more potently decrease vascular inflammation, and reduce CVD mortality, additional immunotherapeutic targets need to be identified. Attractive potential targets are the immune checkpoint proteins, especially co-stimulatory proteins, including CD40.⁷

CD40 and its ligand, CD40L, play a critical role in atherosclerosis by inducing immune cell activation and polarization, which shapes the inflammatory response underlying plaque development and rupture.^{8–10} CD40 is expressed by antigen-presenting cells as well as by non-immune cells, including smooth muscle cells (SMCs), fibroblasts, and endothelial cells,¹¹ while activated T-cells and platelets are the main source of CD40L during atherogenesis.^{11–13} Expression of CD40 (and CD40L) have been reported for almost all cell types in atherosclerotic plaques—human as well as murine. CD40 is expressed by plaque macrophages, endothelial cells, vascular SMCs (VSMCs) and B-cells, while CD40L is

found on T-cells, platelets, endothelial cells, VSMCs, macrophages, and dendritic cells.^{8,10,14–16} CD40-signalling is propagated with the help of tumour necrosis factor (TNF) receptor associated factors (TRAFs). Genetic deficiency, as well as antibody-mediated inhibition of the CD40-CD40L dyad, reduces murine atherosclerosis and induces a clinically favourable stable plaque phenotype, characterized by increased collagen content and reduced necrotic core formation.^{17–21}

Antibody-mediated inhibition of CD40L investigated in a clinical trial setting was complicated by thrombo-embolic events due to the disruption of CD40L- α IIb β 3 interactions in thrombi which compromised the clinical feasibility of this approach.^{22,23} Antibody-mediated targeting of CD40, rather than CD40L, may be an alternative strategy to exploit the therapeutic potential of the CD40-CD40L dyad. However, this approach could result in immunosuppression due to the inhibition of B-cell functioning (e.g. altered immunoglobulin switching) and is, therefore, not feasible for long-term application in patients suffering from CVD.⁸ Recently, we successfully developed small molecule inhibitors specifically targeting the CD40-TRAF6 interaction in macrophages via incorporation into HDL nanobiologics. CD40-TRAF6 inhibition attenuated atherosclerosis in apolipoprotein E-deficient (*Apoe*^{-/-}) mice, limiting signalling interactions downstream of the CD40-TRAF6 pathway [canonical nuclear factor- κ B (NF- κ B) signalling], while leaving CD40-mediated immunity via the CD40-TRAF2/3/5 pathway, including immunoglobulin isotype switching as well as co-stimulation, intact.^{24,25}

These studies highlighted that macrophage CD40 can be considered a major driver of atherosclerosis, and that macrophage CD40 signalling may serve as a therapeutic target using nanobiologics. However, the exact role of macrophage CD40 in atherosclerosis *in vivo* is unknown.

We here investigate myeloid-specific CD40 signalling in experimental atherosclerosis in $ApoE^{-/-}$ mice.

2. Methods

An expanded Methods section is available in the [Supplementary material online](#).

2.1 Animals

$ApoE^{-/-}Cd40^{flox/flox}$ ($CD40^{wt}$) and $ApoE^{-/-}LysM-cre Cd40^{flox/flox}$ ($CD40^{mac-/-}$) mice were generated and bred at the animal facility of the Academic Medical Center, University of Amsterdam, the Netherlands (Janvier Labs, Le Genest-Saint-Isle, France). Mice were humanely euthanized by administration of ketamine (150 mg/kg) and xylazine (10 mg/kg). All animal experiments were conducted at the Amsterdam University Medical Centres, location Academic Medical Centre, University of Amsterdam and approved by the Committee for Animal Welfare of the Academic Medical Center, University of Amsterdam (ethical permit numbers DBC103075-2, DBC265-AF, DBC265-BA, DBC265-AG, DBC265-AX) and the Dutch 'Centrale Commissie Dierproeven' (AVD1180020171666) in accordance with Directive 2010/63/EU of the European Parliament on the protection of animals used for scientific purposes.

2.2 Cell and tissue analysis

Histological, biochemical, flow- and mass-cytometry analyses, as well as computational analyses were performed as described previously by Seijkens et al.²⁴, Cole et al.²⁶, Schindelin et al.²⁷, Schneider et al.²⁸, Dobin et al.²⁹, Li et al.³⁰, Heinz et al.³¹, Love et al.³², Alhamdoosh et al.³³ The datasets generated during and/or analysed during the current study are available from the corresponding author on reasonable request.

Plasma cholesterol (total), HDL-cholesterol, LDL cholesterol, and triglycerides (TGs) were measured by standard enzymatic methods (Roche Diagnostics, Basel, Switzerland) on a COBAS MIRA automated spectrophotometric analyser (Roche Diagnostica). Total cholesterol and TG content in the main lipoprotein classes (VLDL, LDL, and HDL) was also determined using fast protein liquid chromatography as described previously.³⁴

A ProcartaPlex Luminex kit (Affymetrix eBioscience, Vienna, Austria) was used according to the manufacturer's instructions for analysis of secreted cytokines in BMDM culture supernatant as well as in plasma from $CD40^{wt}$ and $CD40^{mac-/-}$ mice.

Total RNA was isolated from $CD40^{wt}$ and $CD40^{mac-/-}$ spleen and lymph, as well as from BMDMs, using a GeneJet RNA Purification Kit according to the manufacturer's instructions (Thermo Fischer Scientific). Complementary DNA (cDNA) was produced by reverse transcription of RNA using the High-Capacity cDNA Reverse Transcription Kit (Thermo Fisher). Quantitative polymerase chain reaction (PCR) was performed with a Sybr Green Master mix (Life Technologies) on a ViiA7 real-time PCR system (Life Technologies). Primers were purchased from Sigma Aldrich and sequences are available upon request.

2.3 Cell culture

Aortic VSMCs were isolated from wild-type and $CD40^{-/-}$ mice—humanely euthanized by carbon dioxide (CO_2) overdose followed by cervical dislocation—by enzymatic digestion and an immortalized murine aortic SMC line (MOVAS; CRL-2797) was purchased from ATCC

(Wesel, Germany). Bone marrow was isolated from femurs and tibiae of $CD40^{wt}$ and $CD40^{mac-/-}$ mice and cells were left to attach and differentiate to bone marrow-derived macrophages (BMDMs) for 7–10 days before being seeded for experiments. Before cell isolation mice were humanely euthanized by CO_2 overdose followed by cervical dislocation.

VSMC collagen synthesis *in vitro* was assessed 72 hours after seeding, using the Sircol™ Soluble Collagen Assay according to the manufacturer's instructions (BioColor, Carrickfergus, United Kingdom).

2.4 Statistical analysis

Statistical comparison between groups was performed using GraphPad Prism software v.8 (GraphPad Software Inc., La Jolla, CA, USA). Data represent mean \pm SD and were analysed by unpaired student's *t*-test or non-parametric Mann–Whitney test where appropriate (depending on normal distribution as assessed via Kolmogorov–Smirnov and Shapiro–Wilk tests. Significance was accepted at the level of $P < 0.05$. Outliers were identified using Grubbs test ($\alpha = 0.05$), and multiple comparisons were corrected for using the Holm–Šidák method.

3. Results

3.1 Generation of mice lacking myeloid CD40 expression

To study the role of myeloid CD40 in atherogenesis *in vivo* in detail, $CD40^{flox/flox}$ and $LysM-cre Cd40^{flox/flox}$ mice were successfully generated on an $ApoE^{-/-}$ background, hereafter referred to as $CD40^{wt}$ and $CD40^{mac-/-}$ mice. BMDMs isolated from $CD40^{mac-/-}$ mice displayed a 70% and 76% reduction of *Cd40* mRNA expression levels under normal and lipopolysaccharide (LPS) stimulated conditions with a corresponding reduction of CD40 protein expression (Figure 1A and B). CD40 expression was not altered in dendritic cells or T-cells in $CD40^{mac-/-}$ mice, nor in neutrophils or monocytes, although baseline expression of CD40 in the latter two cell types was very low (see [Supplementary material online, Figure S1A–C](#)). $CD40^{mac-/-}$ neutrophils did not display altered production of reactive oxygen species (see [Supplementary material online, Figure S1D](#)).

After 14 weeks on a high-cholesterol diet (HCD), $CD40^{mac-/-}$ mice gained on average 6.0 g (± 2.14 g) while their $CD40^{wt}$ littermates gained 8.5 g (± 3.33 g). No differences in plasma lipid profiles were recorded; overall cholesterol and TGs levels, as well as VLDL, LDL, and HDL cholesterol levels were similar in both genotypes (see [Supplementary material online, Figure S2](#)).

3.2 Mice lacking myeloid CD40 expression have a less activated immune profile

Flow cytometric analysis of the blood showed that the fraction of circulating monocytes was decreased, while other circulating/splenic myeloid subpopulations were unaffected in $CD40^{mac-/-}$ compared to $CD40^{wt}$ mice (Figure 1C; see [Supplementary material online, Figure S3A–C](#)). The fraction (as well as absolute number) of $CD3^+$ circulating T-lymphocytes was decreased in $CD40^{mac-/-}$ mice, which was accompanied by a decrease in the fraction of $CD4^+$ effector T-cells and an increase in the fraction of $CD8^+$ naïve T-cells in $CD40^{mac-/-}$ lymph nodes (Figure 1D and E; see [Supplementary material online, Figure S3D–H](#)). Furthermore, the number of circulating $CD4^+$ effector and memory T-cells were decreased (see [Supplementary material online, Figure S3I](#)). Though the lymph nodes and spleen did not show significant differences in other leukocyte subsets between $CD40^{mac-/-}$ and $CD40^{wt}$

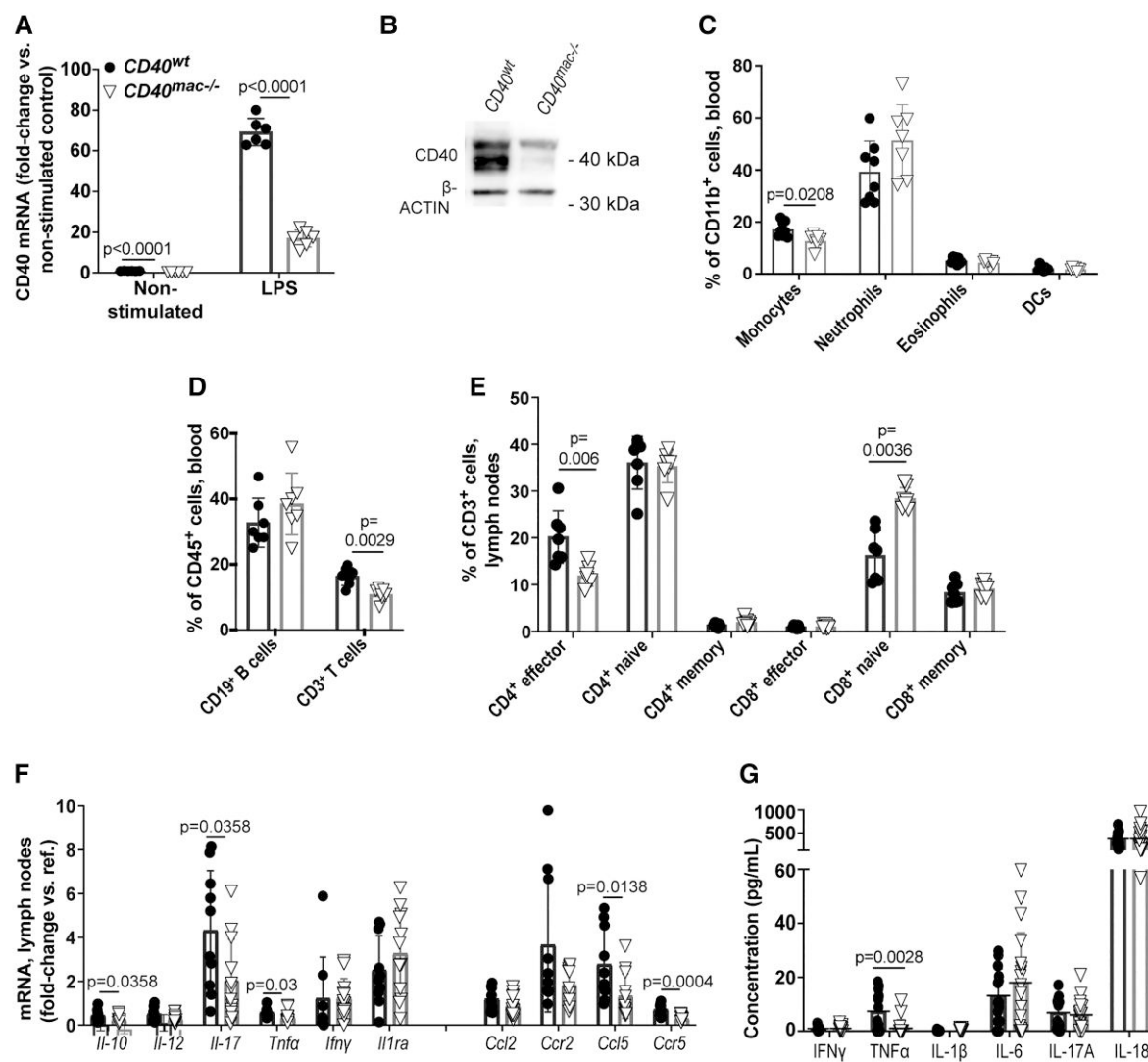


Figure 1 CD40 deficiency and inflammation in $CD40^{mac-/-}$ mice. CD40 expression in LPS or control stimulated BMDMs isolated from $CD40^{mac-/-}$ compared to $CD40^{wt}$ mice (A; $n = 3$ mice; pooled cells, $n = 6$ technical replicates). Western blot showing CD40-expression after stimulation with LPS in $CD40^{wt}$ and $CD40^{mac-/-}$ BMDMs (B; $n = 3$ mice, pooled cells, representative blot shown with an α -tubulin loading control ~ 50 kDa.). Flow cytometric analysis of 22 weeks old $CD40^{wt}$ and $CD40^{mac-/-}$ showing ratios of circulating $CD45^{+}CD11b^{+}Ly6G^{-}$ monocytes, $CD45^{+}CD11b^{+}Ly6G^{+}SiglecF^{+}$ neutrophils, $CD45^{+}CD11b^{+}Ly6G^{-}SiglecF^{+}$ eosinophils, $CD45^{+}CD11b^{+}CD11c^{+}MHCII^{+}$ dendritic cells in (C), ratios of circulating $CD45^{+}CD19^{+}$ B-cells and $CD45^{+}CD3^{+}$ T-cells in (D) and ratios of $CD45^{+}CD3^{+}CD4/8^{+}CD62L^{+/-}CD44^{+/-}$ effector, naïve and memory T-cells in $CD40^{wt}$ and $CD40^{mac-/-}$ lymph nodes (E). Gene expression in $CD40^{wt}$ and $CD40^{mac-/-}$ lymph nodes of chemokines and cytokines analysed by qPCR (mRNA gene expression presented as fold-change against the respective housekeeping gene) is shown in (F), and by Luminex of plasma in (G). $N = 8/6$ for $CD40^{wt}$ and $CD40^{mac-/-}$ mice, respectively, in C; $n = 7$ in (D–E); $n = 10/12$ mice, respectively, in (F), and $n = 14/18$ mice, respectively, in (G). Data is shown as mean \pm SD. Statistical analyses were performed using the unpaired t -test in (A–B) and the Mann–Whitney U test (with multiple comparisons adjusted for using the Holm–Šidák test) in (C–G).

mice (see [Supplementary material online, Figure S4A–J](#)), analysis of the lymph nodes revealed decreased mRNA expression of the inflammatory chemokines and cytokines [$Ccl5$ ($P = 0.0138$), $Ccr5$ ($P = 0.0004$), Tnf ($P = 0.03$), and $Il-17a$ ($P = 0.0358$)] and of anti-inflammatory marker $Il10$ ($P = 0.0358$) in $CD40^{mac-/-}$ mice compared to $CD40^{wt}$ mice ([Figure 1F](#)), whereas concentrations of $TNFA$ and $IL-10$ did not differ on a protein level (see [Supplementary material online, Figure S4K](#)). Finally, the level of plasma $TNFA$ was decreased in $CD40^{mac-/-}$ compared to $CD40^{wt}$ mice ($P = 0.0028$), while cytokine [interferon (IFN)- γ , $IL-1\beta$, $IL-6$, $IL-17A$, $IL-18$] and chemokine (C-X-C motif chemokine ligand

(CXCL) 2, granulocyte colony stimulating factor (G-CSF), CXCL10, C-C motif chemokine ligand (CCL) 2, CCL7) levels were unaffected ([Figure 1G](#); see [Supplementary material online, Figure S4L](#)).

3.3 Macrophage CD40 deficiency reduces atherosclerosis

HCD-fed $CD40^{mac-/-}$ mice displayed a profound reduction in atherosclerotic plaque area in the aortic arch compared to its $CD40^{wt}$ littermates ($P = 0.0134$, [Figure 2A](#)). At first sight, $mac3^{+}$ macrophage

content was similar in atherosclerotic plaques of $CD40^{wt}$ and $CD40^{mac-/-}$ mice (Figure 2B). However, initial plaques of $CD40^{mac-/-}$ mice had a slightly reduced overall macrophage content, whereas the amount of $CD206^+$ cells was increased in advanced $CD40^{mac-/-}$ plaques ($P=0.0495$ and $P=0.0273$, respectively; Figure 2C and D and see Supplementary material online, Figure S5A) and the amount of $CD86^+$ cells had decreased in $CD40^{mac-/-}$ subvalvular plaques ($P=0.050$, see Supplementary material online, Figure S5B). Furthermore, plaques in $CD40^{mac-/-}$ mice displayed a decrease in necrotic core area in comparison to $CD40^{wt}$ mice ($P=0.0122$, Figure 2E). In addition, lipid content was decreased in subvalvular plaques from aortic root sections of $CD40^{mac-/-}$ compared to $CD40^{wt}$ mice ($P=0.0008$, see Supplementary material online, Figure S5C). Plaque content of $CD3^+$ T-cells, smooth muscle α -actin $^+$ SMCs, Ly6G $^+$ neutrophils and TREM2 $^+$ cells, proliferating (Ki67 $^+$), and apoptotic cells (TUNEL $^+$) was unaltered (see Supplementary material online, Figure S5D–I).

One of the key phenotypic features of atherosclerotic plaques of full $CD40$ knockout $ApoE^{-/-}$ mice was a profound increase in collagen content relative to plaque size, corresponding to a reduction in necrosis.²¹ However, we could not detect any changes in the amounts of total collagen (Picro-Sirius Red $^+$), collagen type III or cleaved collagen type I and II (cleavage neo-epitope) in aortic arch plaques of myeloid $CD40$ -deficient mice (see Supplementary material online, Figure S5J–L). As VSMCs, which are the main collagen producing cells in plaques, still express $CD40$ in the $CD40^{mac-/-}$ mice of our model, we investigated the effects of $CD40$ -deficiency on collagen production by VSMCs isolated from full $CD40$ knockout mice. Indeed, we could confirm that collagen production *in vitro* in primary $CD40^{-/-}$ aortic VSMCs was significantly increased compared to wild-type VSMCs ($P=0.0005$; Figure 2F). Furthermore, the secretome of $CD40$ -depleted BMDMs did not appear to affect collagen production in $CD40$ -competent SMCs, as we found similar rates of collagen production by primary wild-type VSMCs cultured in the presence of conditioned media from isolated $CD40^{wt}$ or $CD40^{mac-/-}$ BMDMs either non-stimulated (naïve), classically activated (by LPS) or alternatively activated (by IL-4). However, conditioned media from BMDMs activated by IL-4 was less efficient in promoting VSMC collagen production than conditioned media from non-stimulated or LPS-activated BMDMs ($P<0.0001$ and $P<0.0001$ for IL-4-activation compared to naïve, and $P=0.0002$ and $P=0.0001$ for IL-4- compared with LPS-activation, for $CD40^{wt}$ and $CD40^{mac-/-}$ BMDM conditioned media, respectively; Figure 2G).

Altered capacity for efferocytosis is another macrophage-driven process affecting necrotic core formation. Indeed, we found efferocytosis to be increased in $CD40^{mac-/-}$ compared to $CD40^{wt}$ BMDMs ($P=0.0002$; Figure 2H). These data imply that, while the collagen-rich phenotype observed in fully $CD40$ -deficient mice²¹ is most likely caused by VSMCs, myeloid $CD40$ -signalling determines lesion size, macrophage content and the degree of necrosis, the latter, at least in part, through increased capacity for macrophage efferocytosis.

3.4 Alternatively activated macrophages are abundant in $CD40^{mac-/-}$ atherosclerotic aortas

Within the atherosclerotic aorta, we characterized changes in immune cell populations caused by deficiency of myeloid $CD40$ in detail. Aortas of $CD40^{mac-/-}$ and $CD40^{wt}$ mice were analysed by cytometry by time of flight (CyTOF) analysis after 9 weeks of HCD, signifying an earlier plaque development stage characterized by dynamic changes

and the beginning of necrotic core formation, as well as a pronounced $CD40^{mac-/-}$ phenotype.

A clustering analysis (viSNE) of live $CD45^+$ events, revealed seven leukocyte/cell populations, the largest being the myeloid population (defined as $CD11b^+$). The smaller populations were represented by neutrophils (Ly6G/C $^+$), eosinophils (Siglec-F $^+$), conventional dendritic cells type 1 (cDC1; $CD103^+$), B-cells ($CD19^+$), T-cells ($CD90.2^+$), and natural killer cells ($CD161^+$; Figure 3A; see Supplementary material online, Figure S6A). Within these aortic immune populations, the cell composition was similar in $CD40^{wt}$ and $CD40^{mac-/-}$ mice (Figure 3B; see Supplementary material online, Figure S6B).

Within the $CD11b^+$ (myeloid) population, we identified eight subpopulations: $CD206^+CD169^+CD209b^-$ and $CD206^+CD169^+CD209b^+$ macrophages, $CCR2^+$ macrophages, $CD11c^+$ macrophages, $CD26^-$ and $CD26^+$ cDC2, and Ly6C $^-$ and Ly6C $^+$ monocytes (Figure 4A). Myeloid $CD40$ -deficiency increased the fraction of $CD206^+CD209b^-$ macrophages in the aorta, while the $CD26^+$ cDC2 population ratio was decreased ($P=0.045$ and $P=0.027$ respectively; Figure 4B), suggesting an immune cell profile of a more anti-inflammatory nature that may explain the reduction in atherosclerosis observed in $CD40^{mac-/-}$ mice.

3.5 $CD40$ deficiency promotes alternative macrophage activation

Changes in the macrophage transcriptome caused by deficiency of $CD40$ was further detailed by RNA-sequencing performed on $CD40^{wt}$ and $CD40^{mac-/-}$ BMDMs –after stimulation by the $CD40$ -agonist antibody FGK45. 1307 differentially expressed genes (DEGs) were downregulated and 1463 DEG were upregulated in $CD40^{wt}$ compared to $CD40^{mac-/-}$ BMDMs (Figure 5A; adjusted P -value <0.05).

In $CD40^{wt}$ BMDMs, the top downregulated genes were associated with an alternatively activated (or M2-like) macrophage phenotype and included *Folr2* (folate receptor β , an M2 macrophage marker³⁵), *Thbs1* (thrombospondin-1, reported to limit IL-1 β induction³⁶), *Sdc1* (Syndecan-1, a cell-surface proteoglycan associated with differentiated M2-like macrophages³⁷) and *Tns1* (tensin 1³⁸). $CD40$ -triggering additionally caused a downregulation of *Ccr5* and *Vcam1*, genes involved in migration and adhesion, as well as an increase in *Timp2* [tissue inhibitor of matrix metalloproteinases-2 (MMPs-2)]. Moreover, genes involved in inflammatory responses, including *Mmp14* (active in extracellular matrix turnover³⁹), *Ets2* (a transcription factor required for persistent activation of TNF-alpha by LPS⁴⁰) and *Marco* (M1 macrophage marker;⁴¹ Figure 5A) were upregulated in $CD40^{wt}$ mice.

Ingenuity pathway analysis (IPA) canonical pathways analysis further revealed several dysregulated pathways in $CD40^{mac-/-}$ BMDMs, including $CD40$ signalling, regulation of nuclear factor of activated T-cells and the PI3K-Akt pathway (Figure 5B). In line with the indication of a less inflammatory gene expression profile, multiplex immunoassay showed that $CD40^{mac-/-}$ BMDMs secreted less IFN γ , IL-17A, IL-18, CXCL2, and CXCL10 compared to $CD40^{wt}$ BMDMs (Figure 5C).

3.6 $CD40$ -triggering stimulates classical activation of macrophages

In a reverse experiment we stimulated native and oxidised low-density lipoprotein (oxLDL)-loaded BMDMs with phosphate buffered saline (PBS) or the agonistic $CD40$ antibody FGK45. A profound downregulation was revealed of the alternative activation macrophage marker *Cd206* in lipid-loaded and native BMDMs (adjusted $P=1.14 \times 10^{-7}$

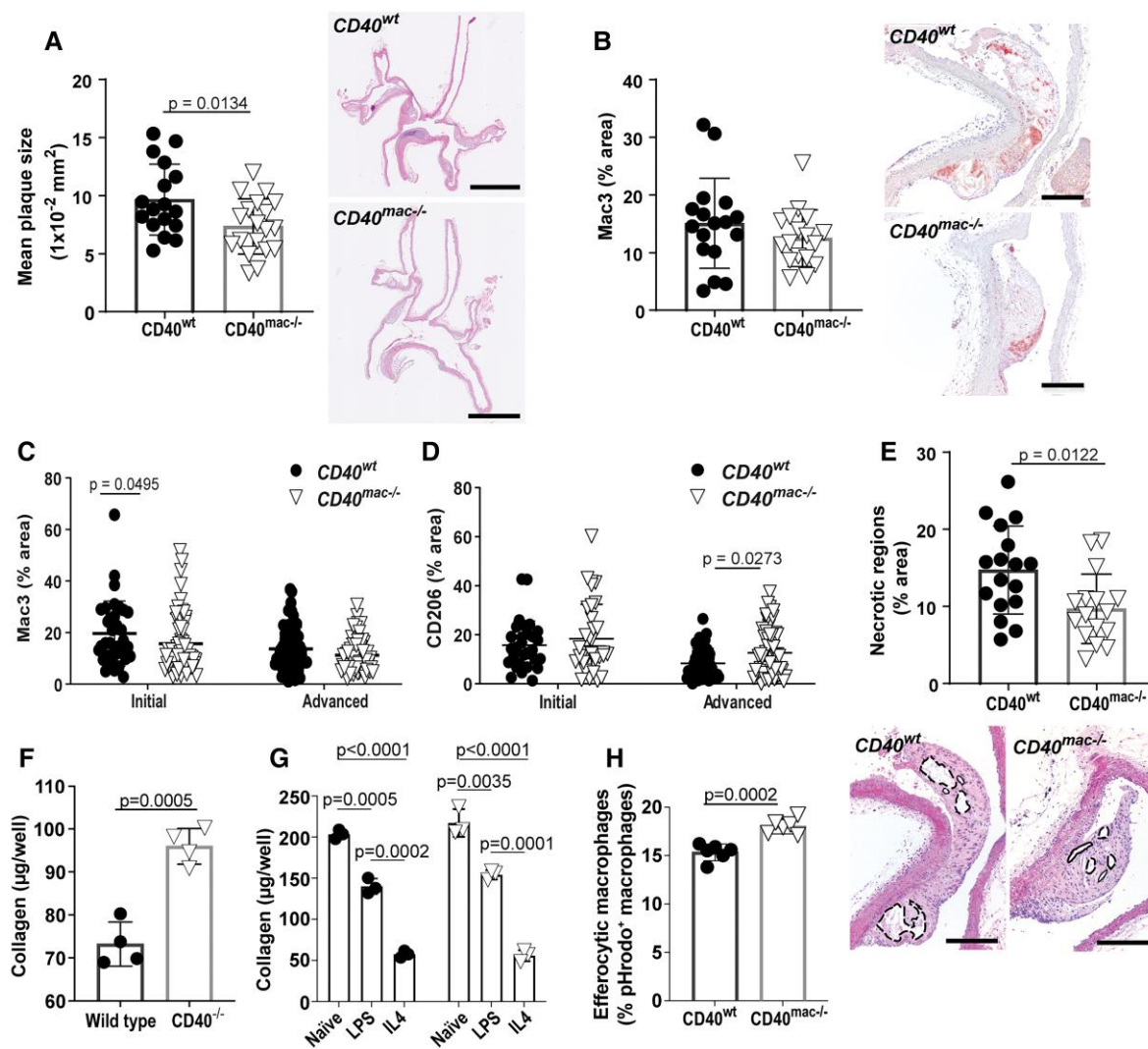


Figure 2 Reduced atherosclerosis in the aortic arch of CD40^{mac-/-} mice. Lesion size (A) and mac3⁺ macrophage content (B) in CD40^{wt} and CD40^{mac-/-} aortic arches. Mac3⁺ macrophages (C) and CD206⁺ cell (D) content was further quantified separately in initial and advanced plaques. Necrotic regions were quantified in CD40^{wt} and CD40^{mac-/-} aortic arches (E; representative haematoxylin & eosin stain with necrotic areas marked by dashed lines). In vitro collagen production by primary murine VSMCs isolated from CD40-deficient and wild-type mice (F) and in immortalized murine VSMCs after stimulation with conditioned media from naive, LPS- or IL4-activated primary CD40^{wt} and CD40^{mac-/-} BMDMs (G). Flow cytometric analysis of efferocytosis in primary bone marrow-derived macrophages isolated from CD40^{wt} and CD40^{mac-/-} mice (H). $N = 19/17$ mice, respectively, in (A), $n = 17$ mice in (B), $n = 110$ CD40^{wt}/142 CD40^{mac-/-} plaques, from $n = 17$ mice in (C), $n = 90$ CD40^{wt}/102 CD40^{mac-/-} plaques from $n = 16/19$ mice, respectively, in (D), $n = 16/17$ mice, respectively, in (E), $n = 4$ replicates in (F), $n = 3$ replicates in (G), and $n = 6$ replicates in (H). Scale bars represent 500 μm in (A) and 200 μm in (B) and (E). Data is shown as mean \pm SD. Statistical tests were performed using the Mann-Whitney U test in (A–E) and the unpaired student's t test in (F–H).

and adjusted $P = 2.15 \times 10^{-7}$, respectively), as well as markers *Cd163* (adjusted $P = 0.0007$) and *cd200r* (adjusted $P = 0.005$) in FGK45- compared to PBS-treated foam cells. Moreover, in foamy as well as in non-foamy BMDMs, classical activation macrophage markers *Inos* (adjusted $P = 7.19 \times 10^{-10}$ and adjusted $P = 0.013$, respectively) and *Cd86* ($P = 4.82 \times 10^{-8}$ and $P = 1.37 \times 10^{-8}$, respectively) were upregulated after CD40 triggering, along with several pro-inflammatory cytokines and chemokines (Figure 6A; see Supplementary material online, Tables SI–SIII).

IPA canonical pathways analysis showed an upregulation of pathways linked to an active immune and inflammatory response, such as IL-8, IL-1 tumor necrosis factor receptor 2, inducible nitric oxide synthase, NF-κB,

and CD40 signalling, in both FGK45-stimulated groups compared to non-stimulated control cells (Figure 6B; see Supplementary material online, Tables SIV and SV). CD40-triggering in BMDMs thus promotes a shift towards a state characterized by classical activation and pro-inflammatory signalling pathways.

3.7 The CD40^{mac-/-} atherosclerotic aorta is less inflamed

The implications of myeloid-specific CD40-deficiency on the transcriptome of atherosclerotic aortas from CD40^{wt} and CD40^{mac-/-} mice was investigated by RNA sequencing. In CD40^{mac-/-} compared to CD40^{wt}

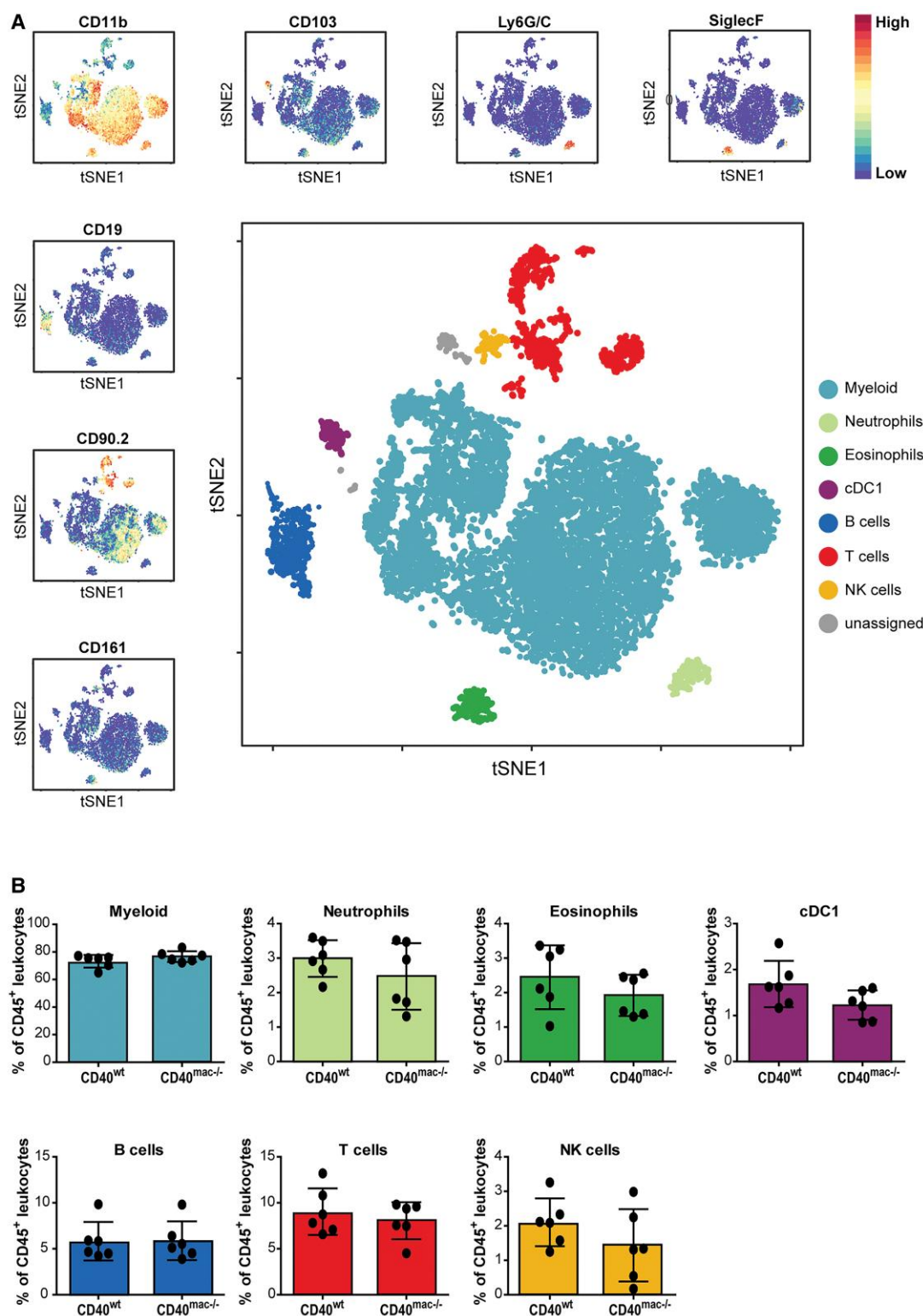


Figure 3 CD45⁺ cell populations in the atherosclerotic aorta of CD40^{wt} and CD40^{mac-/-} mice assessed by CyTOF analysis. Seven CD45⁺ leukocyte populations were identified by viSNE analysis: CD11b⁺ myeloid cells, Ly6G/C⁺ neutrophils, SiglecF⁺ eosinophils, CD103⁺ type 1 conventional dendritic cells (cDC1s), CD19⁺ B-cells, CD90.2⁺ T-cells and CD161⁺ natural killer (NK) cells (A; composite of all cells measured), with cell composition in CD40^{mac-/-} compared to CD40^{wt} mice shown in (B). N = 12/13, respectively for CD40^{wt} and CD40^{mac-/-} mice, with each sample representing two pooled aortas resulting in a final n = 6 samples. Statistical analyses were performed using a multiple t-test with P-values adjusted according to discoveries determined using the two-stage linear step-up procedure of Benjamini, Krieger, and Yekutieli (Q = 1%).

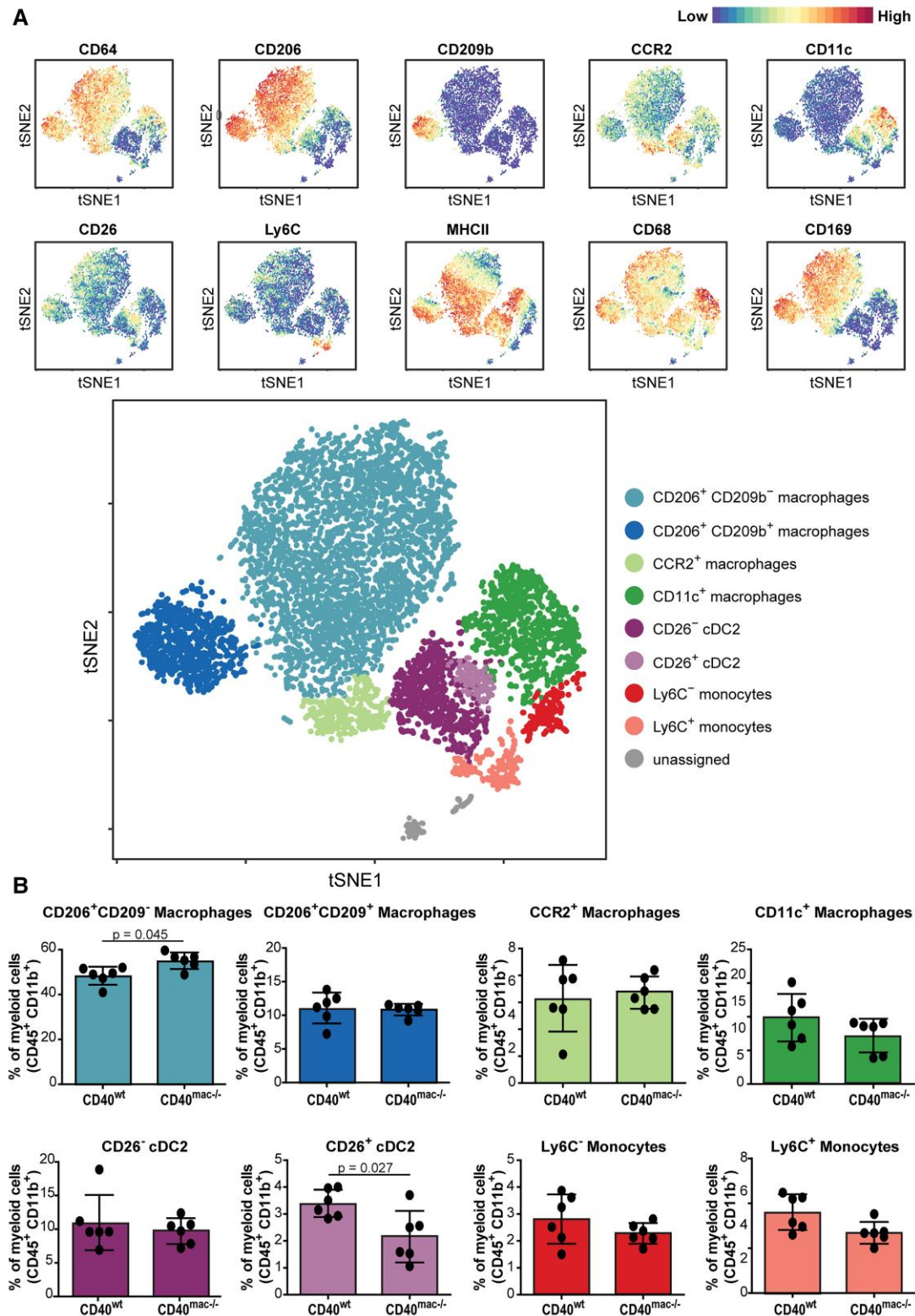


Figure 4 Increased M2 macrophage ratio in CD40-deficient atherosclerotic aortas. Within the CD45⁺CD11b⁺ myeloid cell population in the atherosclerotic aorta eight sub-populations were identified (after neutrophil and eosin populations were subtracted): CD206⁺CD209b⁻ and CD206⁺CD209b⁺ macrophages, CCR2⁺ macrophages, CD11c⁺ macrophages, CD26⁻ and CD26⁺ type 2 conventional dendritic cells (cDC2) and Ly6C⁻ and Ly6C⁺ monocytes (A; composite of all cells measured) with cell composition in CD40^{mac-/-} compared to CD40^{wt} mice shown in (B). $N = 12/13$, respectively, for CD40^{wt} and CD40^{mac-/-} mice, with each sample representing two pooled aortas resulting in a final $n = 6$ samples. Statistical analyses were performed using a multiple t -test with P -values adjusted according to discoveries determined using the two-stage linear step-up procedure of Benjamini, Krieger, and Yekutieli ($Q = 1\%$).

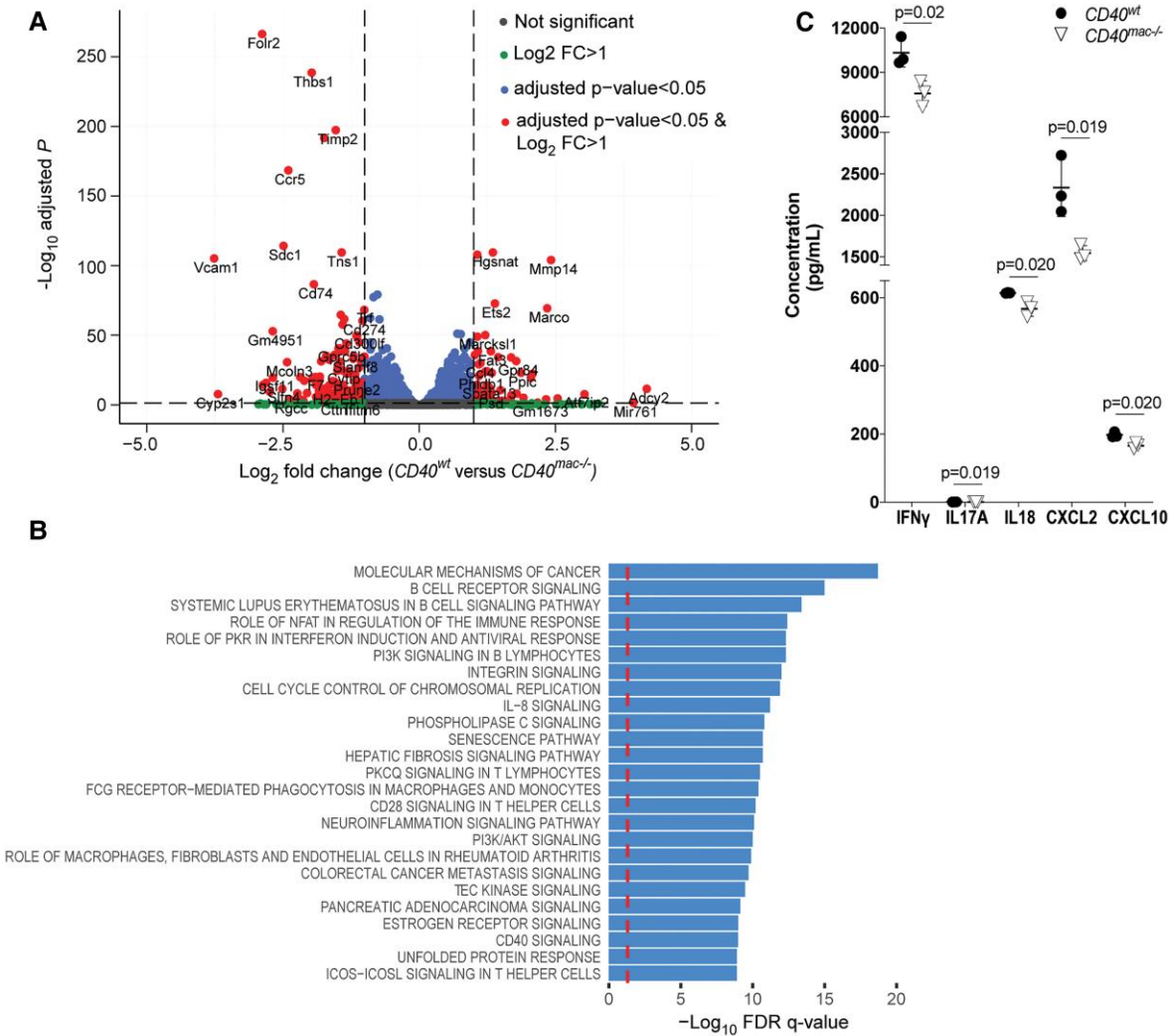


Figure 5 Macrophage genes and pathways affected by CD40-depletion identified by RNA-sequencing. Volcano plot showing *CD40^{wt}* versus *CD40^{mac-/-}* BMDMs (stimulated with FGK45 and IFN γ) (A). Top affected functions in *CD40^{mac-/-}* BMDMs were identified by IPA (B). Levels of IFN γ , IL-17A, IL-18, CXCL2 and CXCL10 were decreased in *CD40^{mac-/-}* compared to *CD40^{wt}* BMDMs (following a stimulation pulse by lipopolysaccharide/IFN γ) as analysed by Luminex (C). Black dashed lines represent cut-off values (adjusted P-value = 0.05, Log₂ fold change = 1). Red dashed lines represent an adjusted P-value = 0.05. N = 3 technical replicates of cells isolated from n = 3 mice. Statistical tests were performed using the Mann–Whitney U test in (C), with data shown as mean \pm SD.

mice atherosclerotic aortas 945 DEGs were upregulated and 797 DEGs were downregulated (Figure 7A; P-value < 0.05).

In *CD40^{mac-/-}* aortas gene set enrichment analysis identified downregulated genes linked to immune pathways and inflammatory responses, such as cytokine and chemokine signalling, while upregulated genes were involved in pathways linked to extracellular matrix (ECM) cell-binding, formation and organization (Figure 7B). The top predicted inhibited upstream regulators (as analysed by IPA pathways analysis) also included pro-inflammatory mediators such as IFN γ , Fas, and miR-199a-5p, while the main activated upstream regulators included IL10RA, transforming growth factor β 1 (TGF β 1), insulin induced gene 1, TGF β ('group'), and SIRT1; all involved in anti-inflammatory pathways (Figure 7C). The propensity of CD40-depleted macrophages to favour alternative activation—as revealed by CyTOF and confirmed by gene expression profiles—thus drives an anti-inflammatory phenotype. The resulting reduction

in systemic and aortic inflammation is ultimately effective in reducing atherosclerosis and necrotic core formation.

4. Discussion

Immune checkpoint proteins play a crucial role in atherogenesis, especially co-stimulatory dyads including CD40-CD40L.⁴² We recently reported that higher plasma levels of soluble CD40 and CD40L are associated with prevalent CVD, with soluble CD40 levels also correlating with carotid atherosclerosis severity and predicting future cardiovascular events.⁴³ Increasing evidence exists that immune checkpoint proteins, i.e. glucocorticoid-induced TNFR-related protein/tumor necrosis factor receptor superfamily member 18 (GITR/TNFRSF18),⁴⁴ CD70,⁴⁵ and CD86,⁴⁶ play a central role in macrophage function. Likewise, CD40—besides its central roles in DC and B-cell maturation

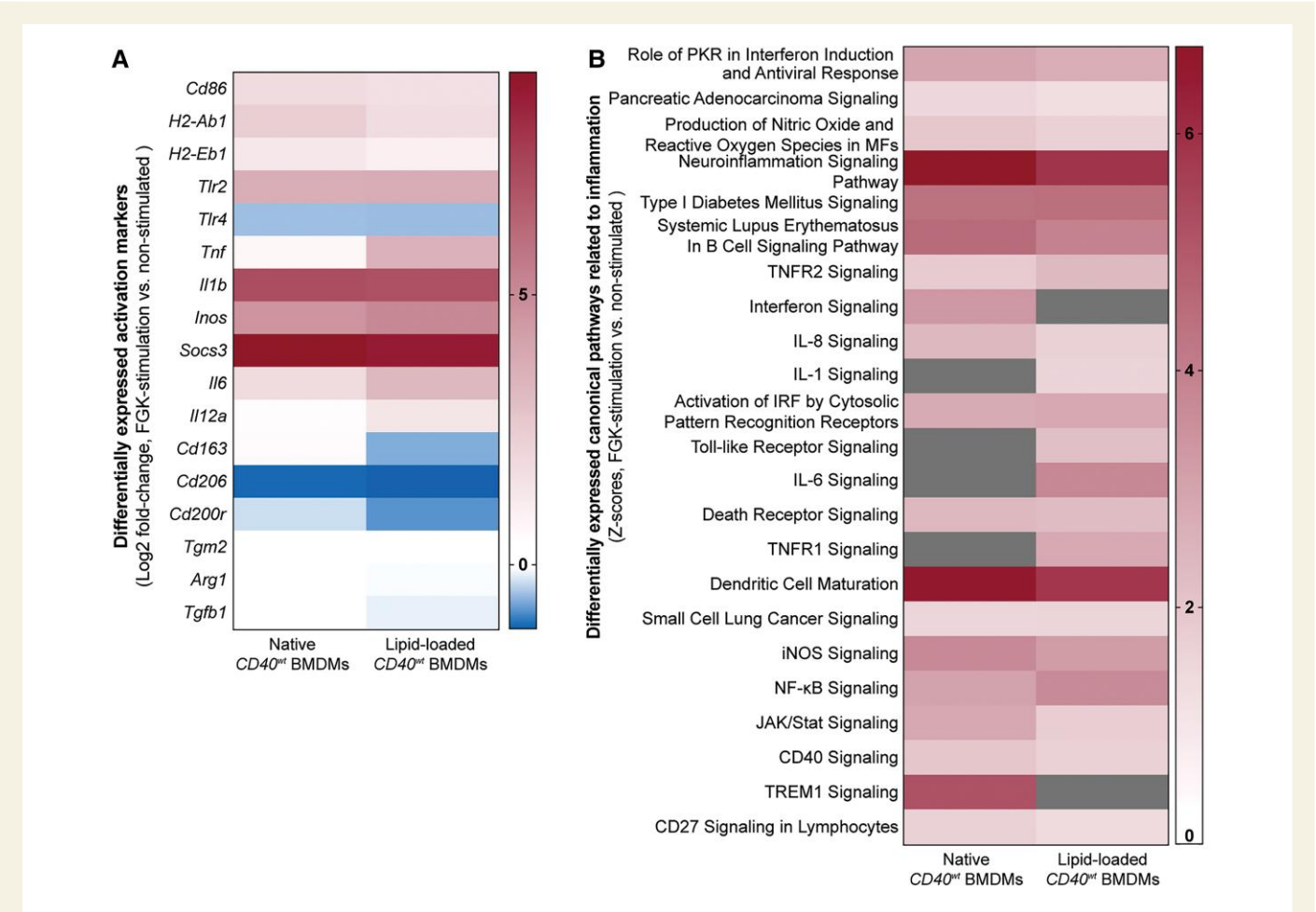


Figure 6 Gene expression resulting from CD40-triggering in native and oxLDL-loaded BMDMs. Gene expression levels relating to classical and alternative macrophage activation are shown in (A), and the main up-regulated pathways identified by IPA pathways analysis are shown in (B). *N* = 3 technical replicates. Grey boxes represent genes with non-significant z-scores or genes lacking sufficient information to produce z-scores.

and adaptive immune response initiation via CD40L binding in CD4⁺ T cells¹¹—also has key functions in macrophages. CD40 triggering in macrophages, via CD40L on T-cells, platelets, endothelial cells, VSCMs and dendritic cells as well as soluble CD40L,^{8,10,14–16} stimulates recruitment of leukocytes via release of chemokines such as monocyte chemoattractant protein-1, macrophage inflammatory protein (MIP)-1α, MIP-1β and regulated upon activation, normal t cell expressed and presumably secreted⁴⁷, aggravates inflammation through cytokine release, including IL-1β, IL-6, IL-12, TNF-α, IFN-γ,^{48–50} and drives T-cell proliferation and T_H1 differentiation.⁸ In atherosclerosis, we could previously show that CD40^{−/−} bone marrow chimeras had reduced atherosclerosis and promoted a stable plaque phenotype²¹—however, others could not.⁵¹ Importantly, the use of irradiation results in the replacement of all bone marrow cells, including B-cells and a subset of DCs, and specific effects of the macrophage on the subsequent atherogenesis are thus not clear. Blocking CD40-TRAF6 signalling systemically leads to a decrease in monocyte recruitment through a reduction in integrin-expression and targeting myeloid CD40 specifically using HDL nanoparticles effectively ameliorated (and stabilized) atherosclerosis,^{24,25} highlighting its promising effect as a therapeutic target. However, though a novel and significant role for immune checkpoint

proteins is emerging in macrophages, until now, the exact role of macrophage CD40 has been unknown.

With this study, we reveal that skewing of macrophage subpopulations towards alternative activation—as demonstrated by mass cytometry and transcriptomic analysis of the atherosclerotic mouse aorta—underlies reduced atherosclerosis resulting from macrophage-specific CD40 depletion. The subsequent CD40^{mac−/−} anti-inflammatory profile manifests as plaques forming of both reduced size and of increased stability, with a higher ratio of CD206⁺ macrophages and less necrosis.

Recently, a meta-analysis of two mass cytometry experiments and nine single cell RNA-sequencing (scRNA-seq) data sets, presented by Zernecke et al.⁵², identified several distinct macrophage subsets in murine atherosclerotic plaques. Four macrophage subsets were identified by Cole et al.²⁶, of which three were also found by Winkels et al.⁵³, all defined by CD11b⁺CD64⁺Ly6C[−] (and using 19 and seven myeloid markers, respectively). The outcome of our CyTOF analysis, using a similar set of markers as Cole et al., is in line with these results: our main macrophage subset discovered to be enhanced by CD40-depletion corresponds to Cole et al.'s²⁶ 'Mac 3' subset (CD11c[−]CD44[−]CD206⁺CD169⁺CD209b[−]). We identified additional subsets corresponding to their 'Mac 1' (CD11c⁺CD44⁺), 'Mac 2' (CD11c^{low}CD44⁺CCR2⁺CD206^{med}CD169[−]) and 'Mac



Figure 7 Genes and pathways of the aorta affected by myeloid-specific CD40-depletion identified by RNA-sequencing. Volcano plot showing *CD40*^{mac-/-} versus *CD40*^{wt} aortas (A). Differentially regulated pathways in *CD40*^{mac-/-} and *CD40*^{wt} aortas were identified by GSEA (B). The top 25 main upstream activated/inhibited regulators were identified by IPA pathways analysis (C; red boxes represent $-\text{Log}_{10}$ *P*-values and grey boxes represent activation z-scores). Black dashed lines represent cut-off values (*P*-value = 0.05, Log_2 fold change = 1). Red dashed lines represent an adjusted *P*-value = 0.05 and green dashed lines represent an unadjusted *P*-value = 0.05. *N* = 5 mice.

4⁺(CD11c[−]CD44[−]CD206⁺CD169⁺CD209b⁺) subsets, which were not affected by CD40-deficiency.

CD206 is widely considered to be a marker for tissue-resident macrophages or the alternatively activated macrophages, characterized as anti-inflammatory with functions directed towards tissue repair and homeostasis.^{54–57} Indeed, increased content of CD206⁺ cells was also immunohistochemically detected in the—compared to *CD40*^{wt}—smaller *CD40*^{mac−/−} plaques. The CD206⁺CD209b[−] macrophage population in our study was also the largest in the atherosclerotic aorta. The proportion of CD206⁺CD169⁺CD209b[−] macrophages reported by Cole et al.²⁶ was decreased in aortas of *ApoE*^{−/−} mice fed a high fat diet—which promotes an inflammatory environment compared to regular chow. That the corresponding macrophage cluster in our *CD40*^{mac−/−} mice did not increase with a HCD compared to the cluster from control aortas is further indication of the lesser inflammatory, anti-atherogenic status resulting from myeloid-specific CD40-depletion. Inclination for CD40-triggering to drive inflammatory macrophage-differentiation was further confirmed *in vitro* in both native and lipid-loaded BMDMs, where transcriptome analysis demonstrated a preference for expression of classically activated, over alternatively activated macrophage markers—along with an overall upregulation of pro-inflammatory pathways.²⁶

Among the CD26[−] and CD26⁺ cDC2 clusters identified by Cole et al.²⁶ in the atherosclerotic aorta, the CD26[−] cDC2 subset was further reported to be decreased in mice receiving an atherosclerotic diet, while the CD26⁺ cDC2 subset—which was of decreased ratio in the *CD40*^{mac−/−} aorta—remained unaltered. The CD26⁺ cDC2s subclass is designated cDC2B and, unlike the anti-inflammatory CD26[−] cDC2A subset, possesses pro-inflammatory potential.⁵⁸ The subclass was recently characterized as non-monocyte-derived inflammatory cDCs with an upregulated expression of cytokines, chemokines, costimulatory molecules and Fc receptors in an IFNAR1 (IFN-α and β receptor subunit 1)-dependent manner.⁵⁹ As their maturation is induced by TLR ligands and type 1 IFN,⁵⁹ their decreased presence in the *CD40*^{mac−/−} aorta is in line with the overall anti-inflammatory profile of these mice.

Five aortic macrophage subsets were proposed in the recent meta-analysis of murine single cell data by Zernecke et al.⁵² using scRNA-seq data sets: resident-like macrophages, Trem2⁺ (triggering receptor expressed on myeloid cells 2) foamy macrophages, inflammatory macrophages, IFN-inducible cell macrophages and cavity macrophages. Of these, a multitude of highly expressed markers by the inflammatory macrophage state are upregulated in native and lipid-loaded BMDMs *in vitro* after CD40-triggering: *Cd14*, *Il-1β*, *Tnf*, *Cxcl-1* and *-2*, and *Ccl-2* and *-3* (representing seven out of eight markers highlighted by this meta-study). In contrast, several markers distinguishing foamy macrophages—among which *Trem2* was identified by transcriptome analysis by Kim et al.⁶⁰ as a common marker for lipid-loaded atherosclerotic macrophages—were downregulated in response to CD40-stimulation: *Cd9*, *Ctsd*, *Fabp5*, in addition to *Trem2* itself. Interestingly, this was not only true for our native BMDMs, but for lipid-loaded macrophages as well. Conversely, expression of the Trem2⁺ foamy macrophage markers—as well as with *Lgals3* (galectin 3, another such marker emphasized by Zernecke et al.⁵²)—were significantly enhanced in CD40-depleted BMDMs (as revealed by RNA-sequencing; data not shown). Kim et al.⁶⁰ further reported that this particular subset of plaque macrophages expresses few inflammatory genes and, thus, concluded that the subset has little involvement in driving plaque inflammation. The overall gene expression profile of CD40-depleted macrophages thus shows clear

similarities to the Trem2^{hi} macrophage state as well as to CD206⁺ resident-like macrophage, while showing little overlap with the inflammatory macrophage substate. The anti-inflammatory profile manifested by our CD40-depleted BMDMs—and, indeed, by the overall diminished and stabilized atherosclerosis displayed by the *CD40*^{mac−/−} atherosclerotic mouse—is in line with a skewing among CD40-depleted macrophages towards an expression profile corresponding to the Trem2⁺ macrophage subset. Importantly, a recent scRNA-seq analysis of human carotid atherosclerotic plaques by Depuydt et al.⁶¹ reports concordance between human and murine plaques with respect to these inflammatory and foamy, anti-inflammatory macrophage subclasses.

Efficient efferocytosis of apoptotic cells—a feature exhibited in particular by alternatively activated macrophages—is atheroprotective and a sign of inflammation resolution, while defective efferocytosis promotes necrotic core formation.^{62,63} The higher efferocytotic efficiency exhibited by CD40-depleted compared to wild type BMDMs is in agreement with this notion, suggesting a greater inclination towards alternative activation and, by extension, increased rate of efferocytosis by CD40-depleted macrophages to be one likely factor underlying reduced necrosis of *CD40*^{mac−/−} plaques. Also consistent with a shift in macrophages towards alternative, anti-inflammatory, activation is the MMP expression profile, with upregulation of *Mmp19* and *Timp2* in *CD40*^{mac−/−} BMDMs, accompanied by a downregulation of *Mmp14*.⁶⁴ Interestingly, MMP14 [together with tissue inhibitor of metalloproteinases 2 (TIMP2)] is essential for activation of pro-MMP2,⁶⁵ and mRNA expression of both *Mmp2* and *-14* is >20-fold higher in vulnerable compared to stable human carotid endarterectomy plaques.⁶⁶ Furthermore, foam cells characterized by high MMP-14 (and low TIMP-3) expression have been reported to be prevalent in rupture-prone atherosclerotic plaques.⁶⁷ The preference towards alternative activation of macrophages was also supported by our observation of reduced gene expression of additional pro-inflammatory mediators, such as *Fas* and *miR-199a-5p*, accompanied by increased expression of anti-inflammatory responses, such as *Lxr*, in the atherosclerotic aorta when myeloid CD40 was lacking.

In contrast to lesions described in the *CD40*^{−/−}*ApoE*^{−/−} mouse and in lesions resulting from CD40-TRAF6 blocking, we did not detect any shifts in the plaque content of α-SMA⁺ SMCs. We did, however, note a general increase in plaque cell density in the *CD40*^{mac−/−} mice (see [Supplementary material online, Figure S5M](#)) that could not be attributed to any of the major plaque cell types with known markers nor to changes in cell viability. This non-classifiable population of cells may represent an increase in the subset of ECM-producing plaque SMCs that no longer express α-SMA after having undergone the phenotypic shift to a more fibroproliferative phenotype. As a matter of fact, SMC lineage-tracing in mice has shown that as many as 82% of plaque SMCs did not express α-SMA.⁶⁸ ScRNA-seq revealed these cells, dubbed ‘fibromyocytes’ by Wirka et al.⁶⁹, to have a transcriptional profile characterized by a striking upregulation of ECM synthesis genes otherwise specific to fibroblasts and to play an atheroprotective role in atherosclerosis. Such pathways, active in ECM formation and organization, were also upregulated in the *CD40*^{mac−/−} aorta. In our study, similar to what has been described by others,⁷⁰ the LysM-cre mouse is able to deplete myeloid specific expression by approximately 70%, which may pose a limitation. However, this level of myeloid CD40 deficiency was sufficient to shift macrophage expression states and successfully reduce atherosclerotic plaque development, while certain additional effects reported for the full CD40 knockout model, such as increased collagen content and reduced MMP expression in plaques, appear to require CD40-depletion in additional cell types. Indeed, we found increased collagen-production in

CD40-deficient VSMCs compared to wild-type VSMCs. Surprisingly, the preference of alternative macrophage activation in *CD40^{mac-/-}* mice may even contribute to decreasing the rate of collagen synthesis by VSMCs, as implied by our observation that conditioned cell culture media from alternatively activated BMDMs has an inhibitory effect on VSMC collagen production *in vitro*. Important to remember is that the development of human plaques spans over several decades compared to a few months in the mouse model. Given similar temporal conditions, the presently found shift in the macrophage gene expression profile towards a larger presence of an alternatively activated subpopulation would likely also lead to long-term plaque stabilization, as a result of a persistently lower grade of plaque inflammation compared to the CD40-competent plaque milieu.

CD40-ligation stimulates production of several pro-inflammatory cytokines and mediators, including TNF α , IL1 α and β , IL-6, IL-8, IL-12, CCL2, -3, -4 and -5, and nitric oxide.⁴⁸ The shift towards an alternatively rather than classically activated macrophage phenotype revealed in our *CD40^{mac-/-}* model consequently appeared in concert with overall milder systemic inflammation in HCD-fed *Apoe^{-/-}* mice as reflected by a decrease in circulating monocytes and CD3⁺ T-cells, as well as plasma TNF α levels. Furthermore, a decrease of CD4⁺ effector T-cells (and increase in CD8⁺ naïve T-cells) was found in lymph nodes, where mRNA for *Tnf α* , *Ccl5*, *Ccr5* and *Il-17a*, and of anti-inflammatory marker *Il-10* were also decreased. These findings are in line with previously reported²⁴ effects on transcriptional and downstream signalling events as a result of blocking CD40-signalling (via TRAF6). CD40-induced phosphorylation of Tak1 and nuclear factor kappa-light-chain-enhancer of activated B cells (NF- κ B) p65 was reduced, but levels of NF- κ B2 p52 or phosphorylation of (extracellular signal-regulated kinase) ERK1/2 (investigated by protein analysis) were unaffected. Further transcriptional analysis confirmed the main affected pathways in CD40-signalling via TRAF6 to be immune reactions and cholesterol biosynthesis. Nonetheless, the observed effects on systemic inflammation were modest and are not expected to affect efficiency or safety of myeloid specific CD40-blocking as a target for immunotherapy against atherosclerosis.

From a therapeutic standpoint, the ability of the current study to achieve such an amelioration of atherosclerosis with only a partial block of myeloid signalling is beneficial, as this allows for a drug-development strategy where preserving low-level CD40-signalling may potentially lead to less systematic side-effects. Other, less narrow or specific, approaches to target CD40-signalling have indeed highlighted the importance of minimizing off-target side effects, such as the increased macrophage infiltration and NF- κ B activation in the kidneys observed in mice after siRNA-silencing of CD40.⁷¹

This is the first study to show that macrophage-specific CD40-depletion reduces atherosclerotic plaque development by shifting macrophage activation towards a more anti-inflammatory state. Our results underscore the high therapeutic potential of targeting CD40 as part of a future atherosclerosis therapy regimen. Using a macrophage-specific approach to blocking CD40-signalling—shown by Seijkens et al.²⁴ and Lameijer et al.²⁵ to be achievable on a practical level—now holds great promise as a feasible tactic of blocking CD40-signalling to reduce and stabilize atherosclerosis. Furthermore, using the novel insights gained by the in-depth characterization of CD40-triggered gene expression in macrophages provided by this study, we shed light on the essential part co-stimulatory signalling in macrophages plays in the disease process.

Supplementary material

Supplementary material is available at *Cardiovascular Research* online.

Authors' contributions

L.A.B., A.S. C.M.v.T., S.A.B.M.A., L.W., J.B., B.W.v.O., M.d.T., L.B., D.J.A., J.H.M.L., A.J., P.D.M., S.G.S.V. and J.v.d.B. conducted experiments/acquired data. C.M., C.M.v.T., D.A., and N.G. contributed to the analysis and/or interpretation of data. A.S. and E.L. designed experiments and analysed/interpreted data and E.L. conceptualized the study. A.S. and L.A.B. wrote the manuscript. All co-authors edited the manuscript.

Conflicts of interest: C.W., D.A., E.L. and N.G. are supported by the Deutsche Forschungs Gemeinschaft (grants CRC1123, A5, SFB 1123, TRR259, SFB1116). E.L. is also supported by the Netherlands CardioVascular Research Initiative, the Dutch Heart Foundation, Dutch Federation of University Medical Centers, the Netherlands Organization for Health Research and Development and the Royal Netherlands Academy of Sciences' for the GENIUS project 'Generating the best evidence-based pharmaceutical targets for atherosclerosis' (CVON2011-19), and the ERC Con grant (CD40-INN). E.L. is also the vice chair at the ESC working group on atherosclerosis, serves on the EAS programme committee and the ATVB awards and programme committee and has received payment or honoraria for lectures at Novartis and Novo Nordisk. The remaining authors have nothing to disclose.

Funding

This work was supported by the Netherlands CardioVascular Research Initiative: the Dutch Heart Foundation, Dutch Federation of University Medical Centers, the Netherlands Organization for Health Research and Development and the Royal Netherlands Academy of Sciences' for the GENIUS project 'Generating the best evidence-based pharmaceutical targets for atherosclerosis' (CVON2011-19). This work was also supported by The Swedish Research Council (2015-00497) and The Swedish Heart and Lung Foundation [20140206; 20150325], the Deutsche Forschungs Gemeinschaft (SFB 1123 to E.L., C.W., and D.A.; TRR259 to E.L. and N.G.; SFB1116 to N.G.) and The European Research Council (ERC Consolidator grant to E.L.).

Data availability

The datasets generated during and/or analysed during the current study are available from the corresponding author on reasonable request.

References

- Libby P, Buring JE, Badimon L, Hansson GK, Deanfield J, Bittencourt MS, Tokgozoglu L, Lewis EF. Atherosclerosis. *Nat Rev Dis Primers* 2019;5:56.
- Ridker PM, Everett BM, Pradhan A, MacFadyen JG, Solomon DH, Zaharris E, Mam V, Hasan A, Rosenberg Y, Iturriaga E, Gupta M, Tsigoulis M, Verma S, Clearfield M, Libby P, Goldhaber SZ, Seagle R, Ofori C, Saklayen M, Butman S, Singh N, Le May M, Bertrand O, Johnston J, Paynter NP, Glynn RJ, Investigators C. Low-dose methotrexate for the prevention of atherosclerotic events. *N Engl J Med* 2019;380:752–762.
- Ridker PM, Everett BM, Thuren T, MacFadyen JG, Chang WH, Ballantyne C, Fonseca F, Nicolau J, Koenig W, Anker SD, Kastelein JJP, Cornel JH, Pais P, Pella D, Genest J, Cifkova R, Lorenzatti A, Forster T, Kobalava Z, Vida-Simiti L, Flather M, Shimokawa H, Ogawa H, Dellborg M, Rossi PRF, Troquay RPT, Libby P, Glynn RJ, CANTOS Trial Group. Antiinflammatory therapy with canakinumab for atherosclerotic disease. *N Engl J Med* 2017;377:1119–1131.
- Tardif JC, Kouz S, Waters DD, Bertrand OF, Diaz R, Maggioni AP, Pinto FJ, Ibrahim R, Gamra H, Kivan GS, Berry C, Lopez-Sendon J, Ostadal P, Koenig W, Angoulvant D, Gregoire JC, Lavoie MA, Dube MP, Rhoads D, Provencher M, Blondeau L, Orfanos A,

- L'Allier PL, Guertin MC, Roubille F. Efficacy and safety of low-dose colchicine after myocardial infarction. *N Engl J Med* 2019;**381**:2497–2505.
5. Nidorf SM, Eikelboom JW, Budgeon CA, Thompson PL. Low-dose colchicine for secondary prevention of cardiovascular disease. *J Am Coll Cardiol* 2013;**61**:404–410.
6. Nidorf SM, Fiolet ATL, Mosterd A, Eikelboom JW, Schut A, Opstal TSJ, The SHK, Xu XF, Ireland MA, Lenderink T, Latchem D, Hoogslag P, Jerzewski A, Nierop P, Whelan A, Hendriks R, Swart H, Schaap J, Kuijper AFM, van Hessen MWJ, Saklani P, Tan I, Thompson AG, Morton A, Judkins C, Bax WA, Dirksen M, Alings M, Hankey GJ, Budgeon CA, Tijssen JGP, Cornel JH, Thompson PL, LoDoCo2 Trial Investigators. Colchicine in patients with chronic coronary disease. *N Engl J Med* 2020;**383**:1838–1847.
7. Lutgens E, Atzler D, Doring Y, Duchene J, Steffens S, Weber C. Immunotherapy for cardiovascular disease. *Eur Heart J* 2019;**40**:3937–3946.
8. Engel D, Seijkens T, Poggi M, Sanati M, Thevissen L, Beckers L, Wijnands E, Lievens D, Lutgens E. The immunobiology of CD154-CD40-TRAF interactions in atherosclerosis. *Semin Immunol* 2009;**21**:308–312.
9. Laman JD, van Meurs M, de Smet BJGL, Schoneveld A. CD40-CD40L interactions in atherosclerosis. *Immunol Today* 1997;**18**:272–277.
10. Mach F, Schönbeck U, Sukhova GK, Bourcier T, Bonnefoy JY, Pober JS, Libby P. Functional CD40 ligand is expressed on human vascular endothelial cells, smooth muscle cells, and macrophages: implications for CD40-CD40 ligand signaling in atherosclerosis. *Proc Natl Acad Sci USA* 1997;**94**:1931–1936.
11. Elgueta R, Benson MJ, de Vries VC, Wasiuk A, Guo Y, Noelle RJ. Molecular mechanism and function of CD40/CD40L engagement in the immune system. *Immunol Rev* 2009;**229**:152–172.
12. Michel NA, Zirikli A, Wolf D. CD40L and its receptors in atherothrombosis—an update. *Front Cardiovasc Med* 2017;**4**:40.
13. André P, Nannizzi-Alaimo L, Prasad SK, Phillips DR. Platelet-derived CD40L: the switch-hitting player of cardiovascular disease. *Circulation* 2002;**106**:896–899.
14. Lutgens E, Lievens D, Beckers L, Donners M, Daemen M. CD40 and its ligand in atherosclerosis. *Trends Cardiovasc Med* 2007;**17**:118–123.
15. Mach F, Schönbeck U, Libby P. CD40 signaling in vascular cells: a key role in atherosclerosis? *Atherosclerosis* 1998;**137**(Suppl):S89–95.
16. Bruemmer D, Riggers U, Holzmeister J, Grill M, Lippek F, Settmacher U, Regitz-Zagrosek V, Fleck E, Graf K. Expression of CD40 in vascular smooth muscle cells and macrophages is associated with early development of human atherosclerotic lesions. *Am J Cardiol* 2001;**87**:21–27.
17. Lutgens E, Cleutjens KBJM, Heeneman S, Koteliensky VE, Burkly LC, Daemen MJAP. Both early and delayed anti-CD40L antibody treatment induces a stable plaque phenotype. *Proc Natl Acad Sci USA* 2000;**97**:7464–7469.
18. Lutgens E, Gorelik L, Daemen MJAP, de Muinck ED, Grewal IS, Koteliensky VE, Flavell RA. Requirement for CD154 in the progression of atherosclerosis. *Nat Med* 1999;**5**:1313–1316.
19. Mach F, Schönbeck U, Sukhova GK, Atkinson E, Libby P. Reduction of atherosclerosis in mice by inhibition of CD40 signalling. *Nature* 1998;**394**:200–203.
20. Schönbeck U, Sukhova GK, Shimizu K, Mach F, Libby P. Inhibition of CD40 signaling limits evolution of established atherosclerosis in mice. *Proc Natl Acad Sci USA* 2000;**97**:7458–7463.
21. Lutgens E, Lievens D, Beckers L, Wijnands E, Soehnlein O, Zernecke A, Seijkens T, Engel D, Cleutjens J, Keller AM, Naik SH, Boon L, Oufella HA, Mallat Z, Ahonen CL, Noelle RJ, de Winther MP, Daemen MJ, Biessen EA, Weber C. Deficient CD40-TRAF6 signaling in leukocytes prevents atherosclerosis by skewing the immune response toward an anti-inflammatory profile. *J Exp Med* 2010;**207**:391–404.
22. André P, Prasad KSS, Denis CV, He M, Papalia JM, Hynes RO, Phillips DR, Wagner DD. CD40L stabilizes arterial thrombi by a beta3 integrin-dependent mechanism. *Nat Med* 2002;**8**:247–252.
23. Kawai T, Andrews D, Colvin RB, Sachs DH, Cosimi AB. Thromboembolic complications after treatment with monoclonal antibody against CD40 ligand. *Nat Med* 2000;**6**:114.
24. Seijkens TTP, van Tiel CM, Kusters PJH, Atzler D, Soehnlein O, Zarzycka B, Aarts S, Lameijer M, Gijbels MJ, Beckers L, den Toom M, Slutten B, Kuiper J, Duchene J, Aslani M, Megens RTA, van 't Veer C, Kooij G, Schrijver R, Hoeksema B, Boon L, Fay F, Tang J, Baxter S, Jongejan A, Moerland PD, Vriend G, Bleijlevens B, Fisher EA, Duivenvoorden R, Gerdes N, de Winther MPJ, Nicolaes GA, Mulder WJM, Weber C, Lutgens E. Targeting CD40-induced TRAF6 signaling in macrophages reduces atherosclerosis. *J Am Coll Cardiol* 2018;**71**:527–542.
25. Lameijer M, Binderup T, van Leent MMT, Senders ML, Fay F, Malkus J, Sanchez-Gaytan BL, Teunissen AJ, Karakatsani N, Robson P, Zhou XX, Ye YX, Wojtkiewicz G, Tang J, Seijkens TTP, Kroon J, Stroes ESG, Kjaer A, Ochando J, Reiner T, Perez-Medina C, Calcagno C, Fisher EA, Zhang B, Temel RE, Swirski FK, Nahrendorf M, Fayad ZA, Lutgens E, Mulder WJM, Duivenvoorden R. Efficacy and safety assessment of a TRA: F6-targeted nanoimmunotherapy in atherosclerotic mice and non-human primates. *Nat Biomed Eng* 2018;**2**:623.
26. Cole JE, Park I, Ahern DJ, Kassireridi C, Danso Abeam D, Goddard ME, Green P, Maffia P, Monaco C. Immune cell census in murine atherosclerosis: cytometry by time of flight illuminates vascular myeloid cell diversity. *Cardiovasc Res* 2018;**114**:1360–1371.
27. Schindelin J, Arganda-Carreras I, Frise E, Kaynig V, Longair M, Pietzsch T, Preibisch S, Rueden C, Saalfeld S, Schmid B, Tinevez JY, White DJ, Hartenstein V, Eliceiri K, Tomancak P, Cardona A. Fiji: an open-source platform for biological-image analysis. *Nat Methods* 2012;**9**:676–682.
28. Schneider CA, Rasband WS, Eliceiri KW. NIH image to imageJ: 25 years of image analysis. *Nat Methods* 2012;**9**:671–675.
29. Dobin A, Davis CA, Schlesinger F, Drenkow J, Zaleski C, Jha S, Batut P, Chaisson M, Gingeras TR. STAR: ultrafast universal RNA-seq aligner. *Bioinformatics* 2013;**29**:15–21.
30. Li H, Handsaker B, Wysoker A, Fennell T, Ruan J, Homer N, Marth G, Abecasis G, Durbin R. Genome project data processing S. The sequence alignment/map format and SAMtools. *Bioinformatics* 2009;**25**:2078–2079.
31. Heinz S, Benner C, Spann N, Bertolino E, Lin YC, Laslo P, Cheng JX, Murre C, Singh H, Glass CK. Simple combinations of lineage-determining transcription factors prime cis-regulatory elements required for macrophage and B cell identities. *Mol Cell* 2010;**38**:576–589.
32. Love MI, Huber W, Anders S. Moderated estimation of fold change and dispersion for RNA-seq data with DESeq2. *Genome Biol* 2014;**15**:550.
33. Alhamdoush M, Law CW, Tian L, Sheridan JM, Ng M, Ritchie ME. Easy and efficient ensemble gene set testing with EGSEA. *F1000Res* 2017;**6**:2010.
34. Fedoseienko A, Wijers M, Wolters JC, Dekker D, Smit M, Huijman N, Kloosterhuis N, Klug H, Schepers A, van Dijk K W, Levels JHM, Billadeau DD, Hofker MH, van Deursen J, Westertep M, Burstein E, Kuivenhoven JA, van de Sluis B. The COMMD family regulates plasma LDL levels and attenuates atherosclerosis through stabilizing the CCC complex in endosomal LDLR trafficking. *Circ Res* 2018;**122**:1648–1660.
35. Puijg-Kroger A, Sierra-Filardi E, Dominguez-Soto A, Samaniego R, Corcuera MT, Gomez-Aguado F, Ratnam M, Sanchez-Mateos P, Corbi AL. Folate receptor beta is expressed by tumor-associated macrophages and constitutes a marker for M2 anti-inflammatory/regulatory macrophages. *Cancer Res* 2009;**69**:9395–9403.
36. Stein EV, Miller TW, Ivins-O'Keefe K, Kaur S, Roberts DD. Secreted thrombospondin-1 regulates macrophage interleukin-1beta production and activation through CD47. *Sci Rep* 2016;**6**:19684.
37. Angsana J, Chen J, Smith S, Xiao J, Wen J, Liu L, Haller CA, Chaikof EL. Syndecan-1 modulates the motility and resolution responses of macrophages. *Arterioscler Thromb Vasc Biol* 2015;**35**:332–340.
38. Bernau K, Torr EE, Evans MD, Aoki JK, Ngam CR, Sandbo N. Tensin 1 is essential for myofibroblast differentiation and extracellular matrix formation. *Am J Respir Cell Mol Biol* 2017;**56**:465–476.
39. Newby AC. Metalloproteinases promote plaque rupture and myocardial infarction: a persuasive concept waiting for clinical translation. *Matrix Biol* 2015;**44–46**:157–166.
40. Wei G, Guo J, Doseff AI, Kusewitt DF, Man AK, Oshima RG, Ostrowski MC. Activated Ets2 is required for persistent inflammatory responses in the Motheaten viable model. *J Immunol* 2004;**173**:1374–1379.
41. Gensel JC, Zhang B. Macrophage activation and its role in repair and pathology after spinal cord injury. *Brain Res* 2015;**1619**:1–11.
42. Kusters PJH, Lutgens E, Seijkens TTP. Exploring immune checkpoints as potential therapeutic targets in atherosclerosis. *Cardiovasc Res* 2018;**114**:368–377.
43. Shami A, Edsfeldt A, Bengtsson E, Nilsson J, Shore AC, Natali A, Khan F, Lutgens E, Gonçalves I. sCD40 levels in plasma are associated with cardiovascular disease and in carotid plaques with a vulnerable phenotype. *J Stroke* 2021;**23**:367–376.
44. Shami A, Atzler D, Bosmans LA, Winkels H, Meiler S, Lacy M, van Tiel C, Ta Megens R, Nitz K, Baardman J, Kusters P, Seijkens T, Buerger C, Janjic A, Riccardi C, Edsfeldt A, Monaco C, Daemen M, de Winther MPJ, Nilsson J, Weber C, Gerdes N, Gonçalves I, Lutgens E. Glucocorticoid-induced tumour necrosis factor receptor family-related protein (GITR) drives atherosclerosis in mice and is associated with an unstable plaque phenotype and cerebrovascular events in humans. *Eur Heart J* 2020;**41**:2938–2948.
45. Winkels H, Meiler S, Smeets E, Lievens D, Engel D, Spitz C, Burger C, Rinne P, Beckers L, Dandl A, Reim S, Ahmadse M, Van den Bossche J, Holdt LM, Megens RT, Schmitt M, de Winther M, Biessen EA, Borst J, Faussner A, Weber C, Lutgens E, Gerdes N. CD70 limits atherosclerosis and promotes macrophage function. *Thromb Haemost* 2017;**117**:164–175.
46. Ley K, Gerdes N, Winkels H. ATVB distinguished scientist award: How costimulatory and coinhibitory pathways shape atherosclerosis. *Arterioscler Thromb Vasc Biol* 2017;**37**:764–777.
47. Mach F, Schönbeck U, Bonnefoy JY, Pober JS, Libby P. Activation of monocyte/macrophage functions related to acute atheroma complication by ligation of CD40: induction of collagenase, stromelysin, and tissue factor. *Circulation* 1997;**96**:396–399.
48. Suttles J, Stout RD. Macrophage CD40 signaling: a pivotal regulator of disease protection and pathogenesis. *Semin Immunol* 2009;**21**:257–264.
49. Munder M, Mallo M, Eichmann K, Modolell M. Murine macrophages secrete interferon gamma upon combined stimulation with interleukin (IL)-12 and IL-18: a novel pathway of autocrine macrophage activation. *J Exp Med* 1998;**187**:2103–2108.
50. Buhtoiarov IN, Lum H, Berke G, Paulnock DM, Sondel PM, Rakhmievich AL. CD40 ligation activates murine macrophages via an IFN-gamma-dependent mechanism resulting in tumor cell destruction in vitro. *J Immunol* 2005;**174**:6013–6022.
51. Bavendiek U, Zirikli A, LaClair S, MacFarlane L, Libby P, Schönbeck U. Atherogenesis in mice does not require CD40 ligand from bone marrow-derived cells. *Arterioscler Thromb Vasc Biol* 2005;**25**:1244–1249.
52. Zernecke A, Winkels H, Cochain C, Williams JW, Wolf D, Soehnlein O, Robbins CS, Monaco C, Park I, McNamara CA, Binder CJ, Cybulska MI, Scipione CA, Hedrick CC, Galkina EV, Kyaw T, Ghoshah Y, Dinh HQ, Ley K. Meta-analysis of leukocyte diversity in atherosclerotic mouse aortas. *Circ Res* 2020;**127**:402–426.

53. Winkels H, Ehinger E, Vassallo M, Buscher K, Dinh HQ, Kobiyama K, Hamers AAJ, Cochain C, Vafadarnejad E, Saliba AE, Zernecke A, Pramod AB, Ghosh AK, Anto Michel N, Hoppe N, Hilgendorf I, Zirlik A, Hedrick CC, Ley K, Wolf D. Atlas of the immune cell repertoire in mouse atherosclerosis defined by single-cell RNA-sequencing and mass cytometry. *Circ Res* 2018;**122**:1675–1688.
54. Stein M, Keshav S, Harris N, Gordon S. Interleukin-4 potentially enhances murine macrophage mannose receptor activity - a marker of alternative immunological macrophage activation. *J Exp Med* 1992;**176**:287–292.
55. Murray PJ, Allen JE, Biswas SK, Fisher EA, Gilroy DW, Goerdt S, Gordon S, Hamilton JA, Ivashkiv LB, Lawrence T, Locati M, Mantovani A, Martinez FO, Mege JL, Mosser DM, Natoli G, Saeij JP, Schultze JL, Shirey KA, Sica A, Suttles J, Udalova I, van Genderachter JA, Vogel SN, Wynn TA. Macrophage activation and polarization: nomenclature and experimental guidelines. *Immunity* 2014;**41**:14–20.
56. Ferrante CJ, Leibovich SJ. Regulation of macrophage polarization and wound healing. *Adv Wound Care* 2012;**1**:10–16.
57. Willemsen L, de Winther MP. Macrophage subsets in atherosclerosis as defined by single-cell technologies. *J Pathol* 2020;**250**:705–714.
58. Shin JY, Wang CY, Lin CC, Chu CL. A recently described type 2 conventional dendritic cell (cDC2) subset mediates inflammation. *Cell Mol Immunol* 2020;**17**:1215–1217.
59. Bosteels C, Neyt K, Vanheerswyngheels M, van Helden MJ, Sichien D, Debeuf N, De Prijck S, Bosteels V, Vandamme N, Martens L, Saey Y, Louagie E, Lesage M, Williams DL, Tang SC, Mayer JU, Ronchese F, Scott CL, Hammad H, Guillems M, Lambrecht BN. Inflammatory type 2 cDCs acquire features of cDC1s and macrophages to orchestrate immunity to respiratory virus infection. *Immunity* 2020;**52**:1039–1056.e1039.
60. Kim K, Shim D, Lee JS, Zaitsev K, Williams JW, Kim KW, Jang MY, Seok Jang H, Yun TJ, Lee SH, Yoon WK, Prat A, Seidah NG, Choi J, Lee SP, Yoon SH, Nam JW, Seong JK, Oh GT, Randolph GJ, Artyomov MN, Cheong C, Choi JH. Transcriptome analysis reveals nonfoamy rather than foamy plaque macrophages are proinflammatory in atherosclerotic murine models. *Circ Res* 2018;**123**:1127–1142.
61. Depuydt MAC, Prange KHM, Slenders L, Ord T, Elbersen D, Boltjes A, de Jager SCA, Asselbergs FW, de Borst GJ, Aavik E, Lonnberg T, Lutgens E, Glass CK, den Ruijter HM, Kaikonen MU, Bot I, Slutter B, van der Laan SW, Yla-Herttuala S, Mokry M, Kuiper J, de Winther MPJ, Pasterkamp G. Microanatomy of the human atherosclerotic plaque by single-cell transcriptomics. *Circ Res* 2020;**127**:1437–1455.
62. Back M, Yurdagul A Jr., Tabas I, Oorni K, Kovanen PT. Inflammation and its resolution in atherosclerosis: mediators and therapeutic opportunities. *Nat Rev Cardiol* 2019;**16**:389–406.
63. Zizzo G, Hilliard BA, Monestier M, Cohen PL. Efficient clearance of early apoptotic cells by human macrophages requires M2c polarization and MerTK induction. *J Immunol* 2012;**189**:3508–3520.
64. Hayes EM, Tsao A, Di Gregoli K, Jenkinson SR, Bond AR, Johnson JL, Bevan L, Thomas AC, Newby AC. Classical and alternative activation and metalloproteinase expression occurs in foam cell macrophages in male and female ApoE null mice in the absence of T and B lymphocytes. *Front Immunol* 2014;**5**:537.
65. Nagase H, Visse R, Murphy G. Structure and function of matrix metalloproteinases and TIMPs. *Cardiovasc Res* 2006;**69**:562–573.
66. Guo ZY, Zhang B, Yan YH, Gao SS, Liu JJ, Xu L, Hui PJ. Specific matrix metalloproteinases and calcification factors are associated with the vulnerability of human carotid plaque. *Exp Ther Med* 2018;**16**:2071–2079.
67. Johnson JL, Jenkins NP, Huang WC, Di Gregoli K, Sala-Newby GB, Scholtes VP, Moll FL, Pasterkamp G, Newby AC. Relationship of MMP-14 and TIMP-3 expression with macrophage activation and human atherosclerotic plaque vulnerability. *Mediators Inflamm* 2014;**2014**:276457.
68. Shankman LS, Gomez D, Cherepanova OA, Salmon M, Alencar GF, Haskins RM, Swiatlowska P, Newman AA, Greene ES, Straub AC, Isakson B, Randolph GJ, Owens GK. KLF4-dependent phenotypic modulation of smooth muscle cells has a key role in atherosclerotic plaque pathogenesis. *Nat Med* 2015;**21**:628–637.
69. Wirka RC, Wagh D, Paik DT, Pjanic M, Nguyen T, Miller CL, Kundu R, Nagao M, Collier J, Koyano TK, Fong R, Woo YJ, Liu B, Montgomery SB, Wu JC, Zhu K, Chang R, Alamprese M, Tallquist MD, Kim JB, Quertermous T. Atheroprotective roles of smooth muscle cell phenotypic modulation and the TCF21 disease gene as revealed by single-cell analysis. *Nat Med* 2019;**25**:1280–1289.
70. Abram CL, Roberge GL, Hu Y, Lowell CA. Comparative analysis of the efficiency and specificity of myeloid-Cre deleting strains using ROSA-EYFP reporter mice. *J Immunol Methods* 2014;**408**:89–100.
71. Hueso M, Casas A, Mallen A, de Ramon L, Bolanos N, Varela C, Cruzado JM, Torras J, Navarro E. The double edge of anti-CD40 siRNA therapy: it increases renal microcapillary density but favours the generation of an inflammatory milieu in the kidneys of ApoE (-/-) mice. *J Inflamm* 2019;**16**:25.